

The application of RPCA on reconstruction of dynamic magnetic resonance image

Yonghong LIU^{1, a}, Jian JIAO^{1, b} and Jicheng CHEN¹

¹EE college Yanshan University Qinhuangdao Hebei province, CHINA

^aliuyh@ysu.edu.cn, ^bnevergamer@hotmail.com

Keywords: RPCA, DMRI, FIST, image reconstruction.

Abstract. The model of robust principal component analysis(RPCA) is built for dynamic magnetic resonance image(DMRI) reconstruction in order to better extract the dynamic part of the cine cardiac tissue. This model decomposes the cardiac magnetic resonance image into sparse part and low-rank part by solving a convex optimization problem mathematically. Fast iterative soft thresholding(FIST) technique is used for faster image reconstruction and simulation results show that clear edge structures with higher spatial and temporal resolution can be guaranteed.

Introduction

Magnetic resonance imaging (MRI) is an inherently slow imaging modality since it is designed to acquire 2-D (or 3-D) k-space data through 1-D free induction decay or echo signals[1,2]. It is the main shortage in many applications especially in the aspect of magnetic resonance imaging. At the same time, slow acquisition process would introduce aliasing artifacts which is also a technical challenge in dynamic magnetic resonance imaging.

In order to increase imaging speed without loss of information, many researchers have applied compressed sensing (CS) approaches which exploit the fact that an image is sparse in some appropriate basis. In k-t SPARSE[3], M. Lustig employ two types of transforms for time-varying cardiac images—a wavelet transform along the spatial dimensions and a Fourier transform along the temporal dimension. In k-t FOCUSS[4], a sparsity constraint is imposed in the temporal transform domain which obtains preferable results in reconstruction of dynamic MRI. In[5], Lingala proposed a k-t SLR method which utilize the sparsity and low-rank of images itself. In[6], Huisu Yoon proposed a motion adaptive spatio-temporal patch-based low rank penalty to capture geometric similarity along motion trajectory as well as within an image frame, this algorithm utilize redundancy of cardiac cine MRI along temporal dimension and is able to effectively reduce noise and aliasing artifacts during reconstruction. Despite all endeavors mentioned above trying to enhance spatial and temporal resolution, they have the similar problems of either large computation or slow convergence which seriously restrict their application on dynamic image reconstruction. Simultaneously, these methods treat the dynamic images as a whole and do not effectively take advantage of different features corresponding to the dynamic part and stationary part for a MRI image.

In this paper, we use the idea of RPCA to build a model of low rank plus sparse, which decomposes the DMRI sequences into dynamic part and static background. We assume the dynamic part constitutes a sparse matrix S , the static background is a low-rank matrix L and regard the reconstruction image X as a superposition of S and L , This model, taking advantage of the sparsity of the motion part and low-rank of stationary part, can effectively extract the dynamic part of the tissue and clearly display the details of a dynamic image, the method of FIST is employed for the reconstruction of cine cardiac magnetic resonance images for better imaging speed and reasonable reconstruction resolution.

Modeling of RPCA

RPCA is widely used in a variety of applications such as image denoising, matrix completion and so on. The idea of RPCA is to decompose the original matrix X into a low-rank part and a sparse part by solving the following optimization problem:

$$\min \text{rank}(L) + \lambda \|S\|_0 \quad \text{s.t. } X=L+S \quad (1)$$

Where $\|\cdot\|_0$ denotes L_0 norm, and λ is regularization parameter

The minimization of rank and L_0 norm is non-convex in the mathematical sense, it is a Non-Deterministic Polynomial(NP) hard problem and need a large amount of calculation. Generally, we make a convex relaxation of Eq. 1, so we obtain Eq. 2, the convex expression:

$$\min \|L\|_* + \lambda \|S\|_1 \quad \text{s.t. } X=L+S \quad (2)$$

Where $\|\cdot\|_1$ denotes L_1 norm and $\|\cdot\|_*$ denotes nuclear norm which is also known as the sum of singular values.

A DMRI normally contains motion part and stationary or approximately stationary background, the dynamic component can be assumed to be sparse or transform-sparse because substantial differences between consecutive frames are usually limited to comparatively small numbers of voxels. Since the background in each frame is approximately stationary, they present highly geometric similarity. If we form a matrix L using these stationary backgrounds, L can be highly correlative.

In summary, RPCA is appropriate for image reconstruction of DMRI. Since the DMRI data are acquired in the spatial frequency domain (k-space) rather than in the image domain, it is necessary to make some revision on Eq. 2. The revised model is as follow:

$$\min \lambda_L \|L\|_* + \lambda_S \|TS\|_1 \quad \text{s.t. } d=E(L+S) \quad (3)$$

where L denotes low-rank matrix, T is sparse operator, and S is sparse matrix. Sparse transform makes S more sparser, which enable higher computational acceleration since fewer coefficients need to be recovered. E denotes spatial encoding operator and d is the undersampled data in k-t space. Regularization parameters λ_L and λ_S are used to keep balance of data consistency and computational complexity between nuclear norm and L_1 norm. High values of λ_L means removing an essentially static background, whereas very low values of λ_L implies more substantial dynamic information in the L component. The selection of λ_S is similar to λ_L .

FIST Reconstruction Algorithm

IST is a common method to solve the optimal problem of RPCA. As an extension of the classical gradient algorithm, it is attractive due to its simplicity and is adequate for solving large-scale problems. although some desired reconstruction images was obtained by IST[7,8], IST is still time-consuming due to its slow convergence. To overcome the shortage, we employ a Fast IST method, which introduces a secondary update content into IST model and greatly reduces reconstruction time. The finite algorithm flow is listed in Table 1.

In this algorithm, $(t_{k-1}-1)/t$ is the step size. The main difference between FIST and IST is that the iterative shrinkage operator is employed on the previous point X_k in IST, whereas FIST uses the usual projection-like step evaluated at an auxiliary point X_k^* very specially constructed in terms of the two previous points X_k and X_{k-1} and an explicit dynamically updated step size $(t_{k-1}-1)/t$. The updating of X_k^* speeds up convergence rate and decreases the number of iterations. The main computational effort in FIST remains the iterative shrinkage operator, and the additional computation in the steps 5 and 6 is marginal. In [9], FIST is proven to converge in function values as $O(1/k)$, whereas IST to converge in function values as $O(1/k^2)$, where k is the iteration counter.

Simulation and analysis

The FIST algorithm was validated by MRI image reconstruction experiments on dynamic cardiac data sets with different downsampled rates. The real cardiac cine data set comes from [4] and it was acquired using a 1.5T Philips scanner at Yonsei University Medical Center, Korea. The FOV (field of view) of the data set were $345 \times 270 \text{ mm}^2$ and matrix size is 256×256 , the sampling trajectory was Cartesian. We compare our proposed algorithm with k-t FOCUSS and IST. All these algorithms are implemented on same MATLAB platform on an Intel i3-4150 processor running at 3.50 GHz with 4 GB RAM. Parameters λ_L and λ_S are set to 0.01 and 0.0025 respectively as in reference [7].

Table 1. Algorithm flowchart of Fast IST for DMRI reconstruction

FIST for reconstruction of DMRI	
1. Initialize: $X_0 = E^*d$, $S_0 = 0$, $t_0 = 1$	
while not converged do	
2. $L_k = \text{SVT}_{\lambda_L}(M_{k-1} - S_{k-1})$	% L: singular-value soft thresholding
3. $S_k = T^{-1}(\Lambda_{\lambda_S}(T(M_{k-1} - S_{k-1})))$	% S: soft thresholding in the T domain
4. $X_k = L_k + S_k - E^*(E(L_k + S_k) - d)$	% Data consistency: subtract residual
5. $t_k = (1 + \sqrt{1 + 4t_{k-1}^2}) / 2$	
6. $X_k^* = X_k + (t_{k-1} - 1) / t_k (X_k - X_{k-1})$	% update
end while	
7. output: L, S	

Performance of these several methods were compared visually and quantitatively and Peak Signal-to-Noise Ratio (PSNR) and Mean Squared Error (MSE) were adopted as numerical evaluation indices. PSNR and MSE are calculated by Eq. 4 and Eq. 5 respectively. In Eq. 4, x_i^* denote reconstruction images, x_i are original images and N is the number of pixels in the images.

$$\text{MSE} = (1/N) \sum (x_i^* - x_i)^2 \quad (4)$$

$$\text{PSNR} = 10 * \log(255/\text{MSE}) \quad (5)$$

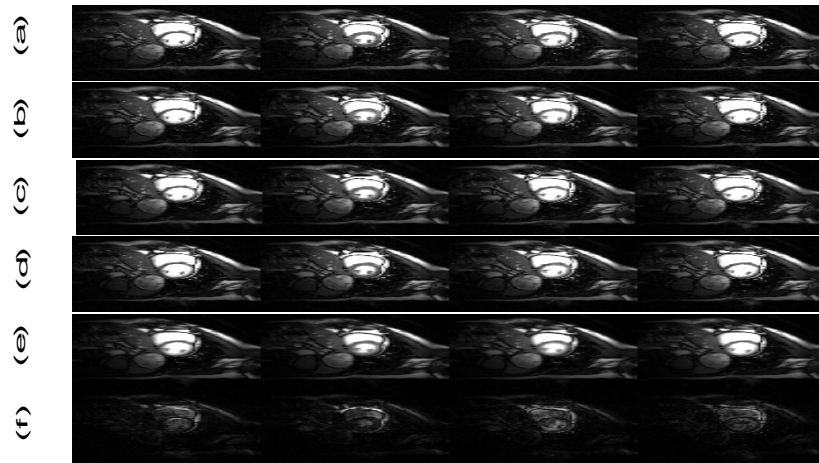


Figure 1. Reconstruction images (downsampling rate: 8)

(a) original images; (b) k-t FOCUSS; (c) IST; (d) FIST

(e) low-rank parts of FIST; (f) sparse parts of FIST

Fig. 1 shows the reconstructed images with downsampling rate of 8, in which (a) denote original images, (b), (c) and (d) are images reconstructed by k-t FOCUSS, IST and FIST respectively and (e), (f) are low-rank parts and sparse parts of (d). We only display some image samples of the 3rd, 9th, 15th, and 21th frame of each kind from left to right. Fig. 2 is the temporal slice profile images, in which (a), (b), (c) and (d) represent the 120th temporal slice profiles of ground-truth, reconstruction

results using k-t FOCUSS, IST and FIST, (e), (f) are the low-rank parts and the sparse parts of (d) respectively. Fig. 2 shows the detailed cardiac part extracted from the whole images. We can see that FIST and IST can produce clearer edge structures whereas k-t FOCUSS can't eliminate the blurring artifacts near edges region. Also, there still remains temporal blurring as shown in Fig. 2(b) while FIST and IST can recover detailed temporal edges. The dynamic part of the images are effectively extracted as shown in Fig. 2(f).

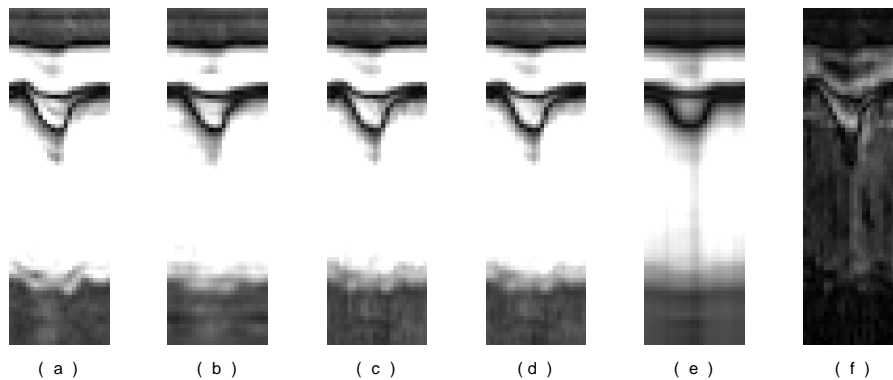


Figure 2. Temporal slice profile images (downsampled rate:8)

(a)original images;(b)k-t FOCUSS;(c)IST;(d)FIST

(e)low-rank parts of FIST;(f)sparse parts of FIST

Our analysis is corroborated by numerical evaluation indices as shown in Table 2 and Fig. 3. Table 2 lists the performance of each algorithm while Fig. 3 shows PSNR values of different algorithms. IST and FIST have higher PSNR values and lower MSE values compared with k-t FOCUSS. Furthermore, Table 2 demonstrates that FIST can greatly reduce the reconstruction time compared with IST due to the decreasing of computation burden.

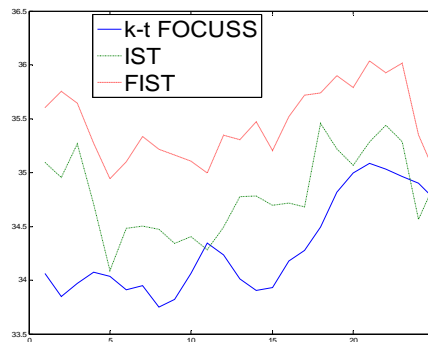


Figure 3. PSNR of different algorithms (downsampled rate:8)

Table 2. Reconstruction performances (downsampled rate:8)

Method	Performance		
	Average PSNR[dB]	Average MSE[10^{-4}]	Time [s]
k-t FOCUSS	34.30	14.65	26.19
IST	34.81	12.74	110.43
FIST	35.46	10.07	71.02

To confirm that the proposed FIST algorithm provides better reconstruction performance than IST and k-t FOCUSS regardless of downsampled rate, Fig. 5 shows reconstruction results with different downsampled rate of 4, in which (a), (b) and (c) denote images reconstructed by k-t FOCUSS, IST and FIST respectively. Table 3 and Fig. 6 show performance of these algorithms.

In Fig. 4, Fig. 5 and Table 3, we can observe the reconstruction results similar to the case of downsampled rate of 8. FIST are able to recover the details in dynamic images especially the edge

structures and has higher PSNR values and spatial and temporal resolution. At the same time, FIST can reduce reconstruction time dramatically compared to IST.

Conclusion

We apply the model of RPCA in reconstruction of magnetic resonance image to better extract the dynamic part of the tissue. Original image is decomposed into the low-rank part and sparse part and FIST algorithm is adopted to solve the convex optimization problem. This method updates the iteration results on the basis of IST and increases convergence rate. Simulation results demonstrate that the proposed algorithm provides clearer edge structures and can effectively extract the dynamic part of the images, higher spatial and temporal resolution can thus be guaranteed.

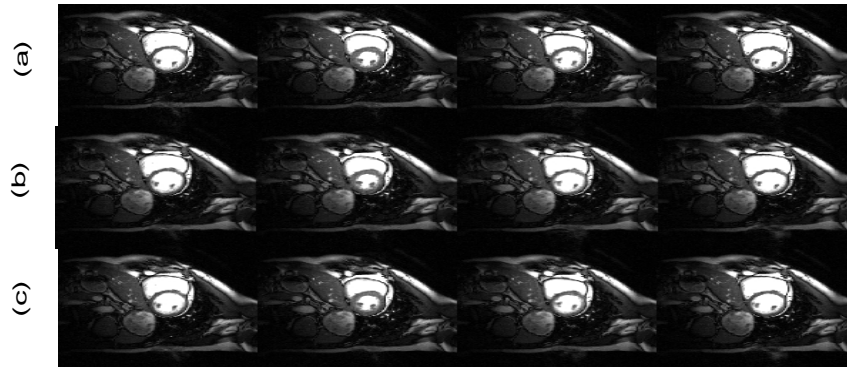


Figure 4. Reconstruction images(downsampled rate:4) (a) k-t FOCUSS;(b) IST;(c) FIST;

Table 3. Reconstruction performances (downsampled rate:4)

Method	Performance		
	Average PSNR[dB]	Average MSE[10 ⁻⁴]	Time [s]
k-t FOCUSS	36.44	5.33	25.83
IST	36.87	4.50	90.70
FIST	37.57	3.24	63.73

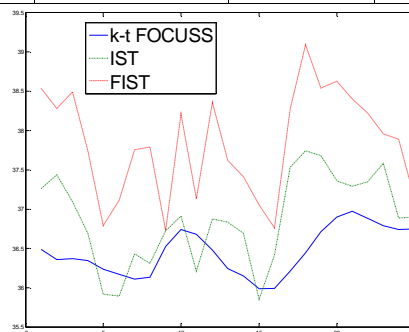


Figure 5. PSNR of different algorithms (downsampled rate:4)

Acknowledgement

This research was financially supported by the National High-Tech Research and Development Program(No.2013AA8093021B). The authors would thank Yonsei University Medical Center of Korea for providing the DMRI data .

References

- [1] M. Lustig, D.L. Donoho, J.M. Santos, J.M. Pauly, IEEE Signal Processing Mag, Vol. 25 No. 2 (2008), p. 72–82.

- [2] M. Lustig, D. Donoho, J. Pauly, *Magnetic Resonance in Medicine*, Vol. 58 (2007), p.1182–1195
- [3] M. Lustig, J. Santos, D. Donoho, J. Pauly, “kt SPARSE: High frame rate dynamic MRI exploiting spatio-temporal sparsity, in *Proceedings of. 13th Annu. Meet. ISMRM*, Seattle, WA, 2006, p. 2420-2425.
- [4] H. Jung, K. Sung, K. Nayak, *Magnetic Resonance in Medicine*, Vol. 61 (2009), p. 103-116.
- [5] S.G. Lingala, Y. Hu, E.DiBella, M. Jacob, *IEEE Transactions on Medical Imaging*, Vol. 30 (2011), p.1042–1054
- [6] H. Yoon, K. S. Kim, J.C. Ye, *IEEE Transactions on Medical Imaging*, Vol. 33 (2014), p.2069-2085.
- [7] R. Otazo, E. Candes, D.K. Sodickson, *Magnetic Resonance in Medicine.*, Vol. 73 (2015), p. 1125–1136.
- [8] R. Otazo, D.K. Sodickson, E. Candes. Low-rank + sparse (L+S) reconstruction for accelerated dynamic MRI with separation of background and dynamic components, in *Proceedings of. SPIE 8858, Wavelets and Sparsity XV*, 2013, p.8858.
- [9] A. Beck, M. Teboulle, *SIAM Journal on Imaging Sciences*, Vol. 2 (2009), p. 183-202.